INTERNATIONAL JOURNAL OF SUSTAINABLE CONSTRUCTION ENGINEERING AND TECHNOLOGY
VOL. 14 NO. 1 (2023) 226-240

IJSCET

http://publisher.uthm.edu.my/ojs/index.php/ijscet

ISSN : 2180-3242 e-ISSN : 2600-7959

International Journal of Sustainable Construction Engineering and Technology

Seismic Performance of X-Braced Frame with Vertical Link Beam (XBF-VLB)

Pouria Nouria[1*]

[1]Department of Civil Engineering,
Qazvin Branch, Islamic Azad University, Qazvin, IRAN

*Corresponding Author

DOI: https://doi.org/10.30880/ijscet.2023.14.01.020
Received 03 September 2022; Accepted 08 January 2023; Available online 14 February 2023

Abstract: X-braced Frames(XBFs), one of the most prevalent lateral load-resisting structures, has low energy dissipation and ductility. This study investigates the behavior of a single-story, single-span X-braced frame equipped with a Vertical Link Beam (XBF-VLB) under monotonic and cyclic loading using the nonlinear finite element technique in the Abaqus software and validated with experimental data. The VLBs were positioned where the bracing members were connected to the beam in double, single, and wide forms. The impacts of the length, depth, and the number of links, stiffeners, and other VLB section parameters were assessed. The A36 steel ductile damage method (DDM) estimated the damage of the main structural members, such as bracing members. The results revealed that X-braced frames with single, double, and wide form Vertical Link Beams (XBF-VLBs) performed better under cyclic and monotonic loading than X-braced frames without Vertical Link Beam (XBFs). Likewise, because the bracing members did not buckle in the XBF-VLB specimens, there was no rapid loss in the stiffness and strength of the X-braced frames. Also, the results of the cyclic loading of the XBF-VLB specimens demonstrated that no rapid drop in stiffness or strength was detected due to no buckling of the bracing members under the cyclic loading, as was the case with the monotonic loading. Additionally, compared to the XBF specimens, the drifts corresponding to the first plastic hinges of the XBF-VLB specimens show that the bracing members experienced nonlinear deformation at greater drifts, with the plastic hinges created in them at bigger displacements. According to the cyclic loading results, the VLB also reduced Von Mises stress and damage in the bracing members of the XBF-VLB specimens. Moreover, the ultimate von Mises stress reduction in the bracing members of the models with VLBs equals 33%, which prevents buckling.

Keywords: X-Braced frame, nonlinear finite element method, structural fuse, Vertical Link Beam (VLB), energy dissipation

1. Introduction

A Concentrically Braced Frame (CBF) is often used as a potential lateral load-resisting solution in seismic areas due to its stiffness and strength. For CBFs, the brace components are developed to deform inelastically and exhibit post-buckling behavior to absorb a significant percentage of the energy like a Structural Fuse (SF). On the other hand, the gusset plates are developed to withstand the loads exerted by the braces and maintain the significant inelastic deformation throughout earthquake occurrences [1]. Typical bracing systems have been modified several ways to increase their ductility and energy dissipation capability. The objective of the majority of modified approaches is to focus the significant inelastic deformation onto a secondary element. In the early 1970s, extensive research on EBFs was done. These braced frames are extensively used in earthquake-resistance systems. The EBF is a braced frame; one

*Corresponding author: p.nouri@qiau.ac.ir

side of the brace is attached to a beam to provide enough performance in the case of strong earthquake occurrences, and the other is attached to a column. In this system, the link beam works as a structural fuse by transferring moment and shear forces to the structure [2-5] .The seismic performance and design process of EBF is now the subject of much research [6-9].

The effect of a link over strength on the seismic performance of EBFs made in accordance with capacity design guidelines was examined, Furthermore, the results indicated that the seismic response of EBFs is usually impacted by the link strength variables and the dynamic characteristics of Movements caused by earthquakes [10]. Based on the seismic performance of the link, the seismic behavior of EBF was investigated. Irrespective of connection length, the results indicated that the most likely location for EBF system to fail is around the groove on the flange [11].

Utilizing static and dynamic nonlinear analyses, it is shown that the global method is frequently the reason for the collapse, matching the suggested concept design. Consequently, this method may be developed in the earthquake-resistant design of buildings. The vast majority of inelastic dynamic simulations have highlighted the significant effect of the link-beam over strength factor on the seismic performance of conventional eccentrically braced structures [12, 13].

The Reduced Beam Section (RBS) function connecting lengthy link beams was investigated; Yield incidence might be delayed in the link-beam (prior to reaching a middle placement of RBS at the column's side) around10% more than the projected plastic valence. In addition, RBS separates the plastic hinge from the link connections [14]. Bar Fuse Damper (BFD) is a novel passive damper, which has been evaluated in the braced frame. This damper has several steel rods, which dissipates seismic energy by deforming the cross-section of the rods. Moreover, the rods are replaceable, which is an advantage of BFD [15, 16]. Daneshmand and Hashemi [17] investigated 68 connections using the finite element method to evaluate the primary behavior of medium and lengthy links in EBFs. They discovered that certain medium links lacked the needed rotation capability. In addition, Researchers examined the impact of link length on the behavior of EBFs and found that long links had worse ductility and energy dissipation valence than short link beams [18, 19].

Zahrai and Tabar [20] performed a numerical analysis of a shear panel system that functions as a ductile link beam linking bracing to the floor beam. The research focused on crucial factors affecting the cyclic behavior of frames braced by SPSs, such as the cross-sectional characteristics of SPSs and the length of the links. The findings suggested that the shear panel's length substantially affects the cyclic performance of these systems. The hysteretic response of eccentrically braced frames with the zipper-strut upgrade was analyzed, and results indicated that the zipper-strut-equipped system exhibited a greater propensity to create shear links, resulting in a higher absorption valence in the plastic area [21].

Montuori et al. [22] established a comprehensive and extensive design approach for MRF–EBF dual systems, assuming all regularly used brace designs guarantee the construction of a global type collapse mechanism.

Using the nonlinear finite element method in the Abaqus software[23], the present study investigates the behavior of a single-story, single-span X-braced frame equipped with a Vertical Link Beam (XBF-VLB) under monotonic and cyclic loading. Braced frame systems, especially X-braced frames (XBFs), have high stiffness. As shown in Fig. 1, during severe earthquakes, the bracing members undergo buckling and damage immediately after yielding. In this numerical study, a Vertical Link Beam (VLB) was used to prevent buckling in bracing members at large drifts through energy dissipation in lateral loading. The VLBs, in double, single, and wide forms, were placed at the point where bracing members were connected to the beam. The effects of VLB section properties, such as stiffeners and length, depth, and number of links, were evaluated.

Fig 1 - Buckling of bracing members of the X-braced Frame in the 2017 Sarpol Zahab earthquake

2. Numerical Modeling

2.1 Model Geometry

In the numerical study, a finite element model of a X-braced frame equipped with a Vertical Link Beam (XBF-VLB) was developed to investigate the impacts of different parameters on the seismic behavior of the system. To this end, 12 single-story, single-span X-braced frames, with span length of 5150 mm and 3100 mm height, equipped with Vertical Link Beams were used. According to Fig. 2, the models included three general Vertical Link Beam (VLB) installation forms in the point where bracing members were connected to the beam: 1) X-braced frame with a single Vertical Link Beam (XBF-VLB$_{(S)}$), 2) X-braced frame with pair Vertical Link Beams (XBF-VLBs$_{(P)}$), 3) X-braced frame with a Vertical Link Beam with a wide web (XBF-VLB$_{(W)}$). The impacts of parameters like the length of the VLB and stiffeners were taken into account for each of the mentioned modes. A X-braced frame model with no Vertical Link Beam (XBF) was also developed to compare its results with those of the models equipped with VLBs in the Abaqus software. Overall, 12 models of X-braced frames equipped with Vertical Link Beams (XBF-VLBs) and one without any Vertical Link Beam (XBF) were modeled in the Abaqus software[23]. As shown in Table 1, IPB140 and IPE300 were used as beam and column sections, respectively. A 2UNP140 section, consisting of two U-sections in front of each other, was used for bracing members in the models, and an IPE240 section was employed for the VLBs. All details of the X-braced frame without Vertical Link Beam (the base model) were designed based on the seismic design requirements of AISC[24].

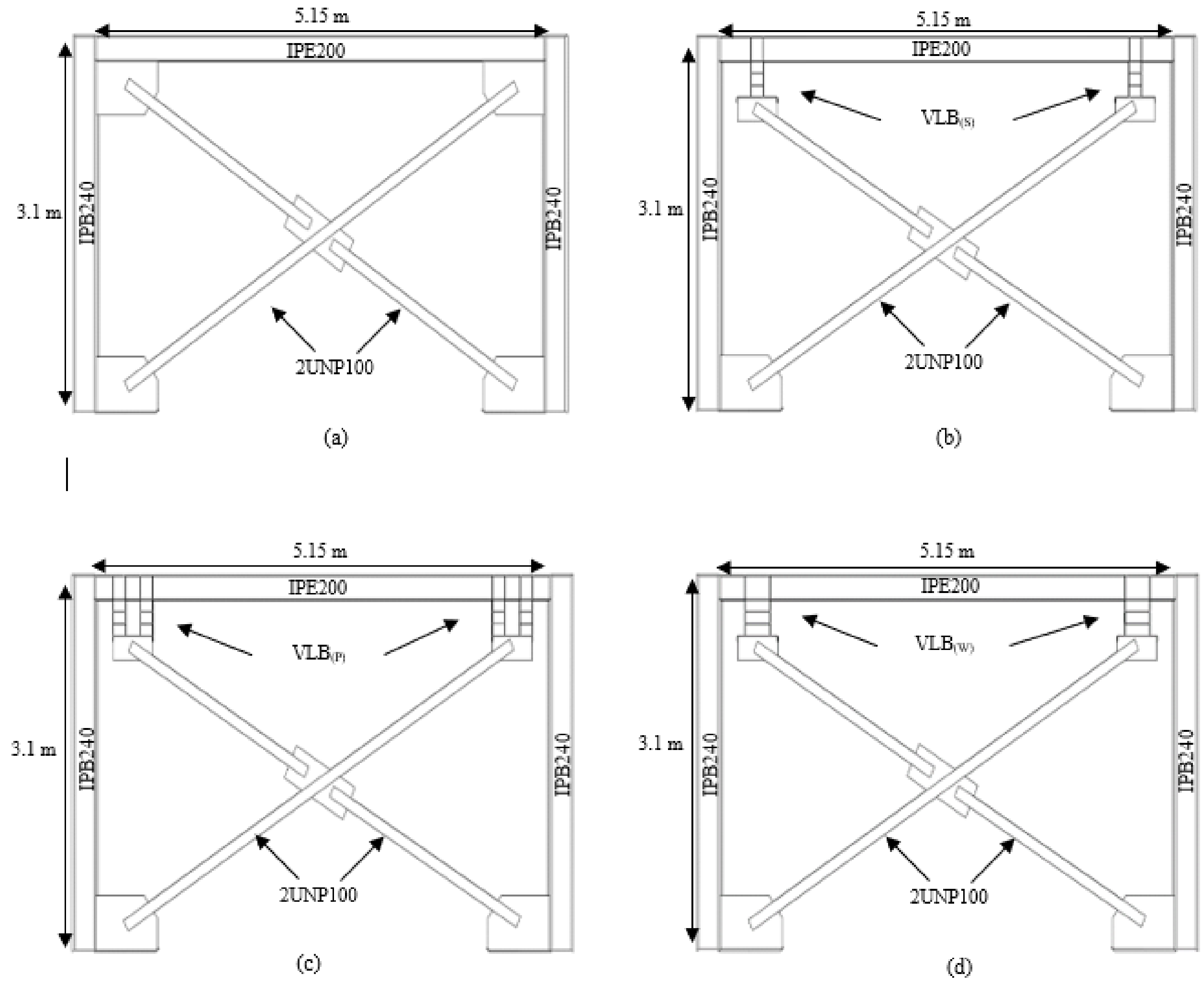

Fig 2 – (a) X-braced frame (XBF); (b) X-braced frame with Single Vertical Link Beam (XBF-VLB$_{(S)}$); (c) X-braced frame with Pair Vertical Link Beams (XBF-VLBs$_{(P)}$); (d) X-braced frame with Wide Vertical Link Beams (XBF-VLB$_{(W)}$)

Table 1 - Dimensions and design characteristics of structural members in models

Models	Type of VLB	Specifications of samples	Beam		Columns		Braces		Vertical Link Beam (VLB)		
			Section	L(mm)	Section	L(mm)	Section	L(mm)	Section	L(mm)	Stiffener
Model 1	**-**	**XBF**	IPE200	5150	IPB240	3100	2UNP100	5100	-	-	-
Model 2	Single	**XBF-VLB$_{(S)}$**	IPE200	5150	IPB240	3100	2UNP100	5100	IPE140	200	NO
Model 3		**XBF-VLB$_{(S)}$**								200	YES
Model 4		**XBF-VLB$_{(S)}$**								300	NO
Model 5		**XBF-VLB$_{(S)}$**								300	YES
Model 6	Pair	**XBF-VLB$_{(P)}$**	IPE200	5150	IPB240	3100	2UNP100	5100	IPE140	200	NO
Model 7		**XBF-VLB$_{(P)}$**								200	YES
Model 8		**XBF-VLB$_{(P)}$**								300	NO
Model 9		**XBF-VLB$_{(P)}$**								300	YES
Model 10	Wide	**XBF-VLB$_{(W)}$**	IPE200	5150	IPB240	3100	2UNP100	5100	IPE140(h_w=280)	200	NO
Model 11		**XBF-VLB$_{(W)}$**								200	YES
Model 12		**XBF-VLB$_{(W)}$**								300	NO
Model 13		**XBF-VLB$_{(W)}$**								300	YES

2.2 Loading

Pinned supports were used as boundary conditions in the bottom of the columns of the base model and the models equipped with Vertical Link Beams. Moreover, the beam displacement in the perpendicular direction was prevented. The displacement-control lateral load was applied to the two tops of the columns of the models. The loading included pushover analysis with a monotonic loading up to the drift of 4% and a cyclic loading according to AISC[24]. The cyclic loading also continued up to the drift of 4% to properly show the damage and buckling in the bracing members of the base model. Fig. 3 depicts the diagram of the cyclic loading protocol used in the study.

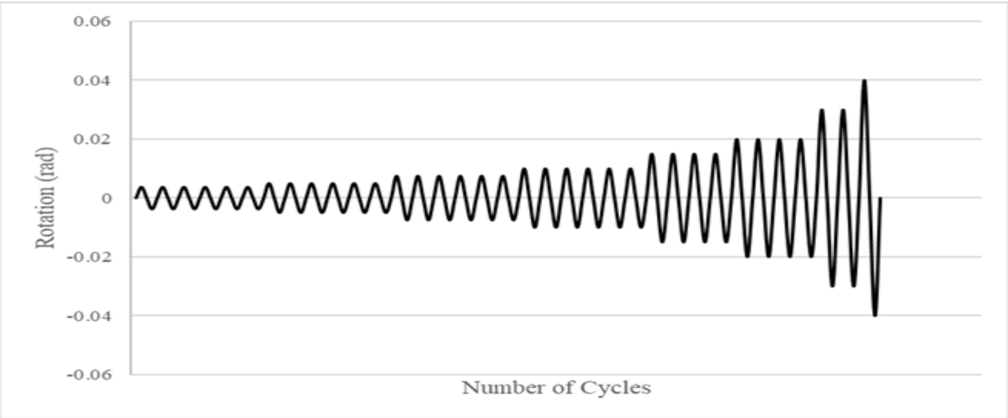

Fig 3 - AISC loading protocol [24]

2.3 Meshing Model

Four-node shell elements from the element library of the Abaqus software[23] were employed to model the main members of the X-braced frame, such as beams, columns, bracing members, and VLBs. These elements have six degrees of freedom in each node and can well depict large deformations in these members. Moreover, in order to show the ductile damage method, the element removal option was defined in the main members, like the bracing members. The impact of large deformations was also taken into consideration in the modeling.

2.4 Material Properties

Given the nonlinear deformations in the main members of the X-braced frame, especially bracing members, the nonlinear behavior of steel was used to define steel properties. The hardening behavior of materials can be divided into three groups: isotropic, kinematic, and a combination of both. In isotropic hardening, the yielding surface remains almost the same and is expanded or shrunk around the center. In other words, no change occurs in its shape or center. Isotropic hardening can be linear or nonlinear. Meanwhile, in kinematic hardening, the center is changed, while no change occurs in the plate size or shape [25]. In phenomena like the Bauschinger effect (the impact of reduced yield stress after plastic deformation), cyclic hardening, cyclic creep, and relaxation, it is better to use a nonlinear combination of isotropic-kinematic hardening.

Accordingly, for precise modeling of the material behavior under cyclic loading, in the present study, a combination of nonlinear isotropic-kinematic hardening, along with the von Mises yield stress, was used to evaluate plastic deformations of the main members, such as bracing members. The A36 steel [26] with a yield stress of 268 MPa, Young's modulus of 200 GPa, and a Poisson's ratio of 0.3 was used to define the materials of the main members of the X-braced frame, such as beams, columns, bracing members, and VLBs. In order to represent damages in the main members of the X-braced frame, the ductile damage method with the damage parameters of A36 steel was used[27].

2.5 Validation

In order to validate the results obtained from the Abaqus finite element software, the experimental specimens of a link beam and a concentrically braced frame were modeled as described in the following.

2.5.1 Validation of the Concentrically Braced Frame

In order to validate the X-braced frame modeling, specimen F4, one of the specimens of concentrically braced frames tested in a laboratory[28], was modeled and subjected to cyclic loading in the Abaqus software[23]. This frame was made up of a W460×128 beam section, a W310×143 column section, and 25.4×50.8 bracing sections. Moreover, the properties of A572 steel were used for the main members of the specimen. Fig. 4 makes a comparison between the cyclic curves of the experimental specimen and the numerical model. As can be seen, the results are close, and the maximum base shear values in the numerical and experimental models are 649.31 and 667.68 KN, showing a small difference of 3%. The deformation and buckling values in the bracing members of the two models in the 19th cycle are also compared in Fig. 5.

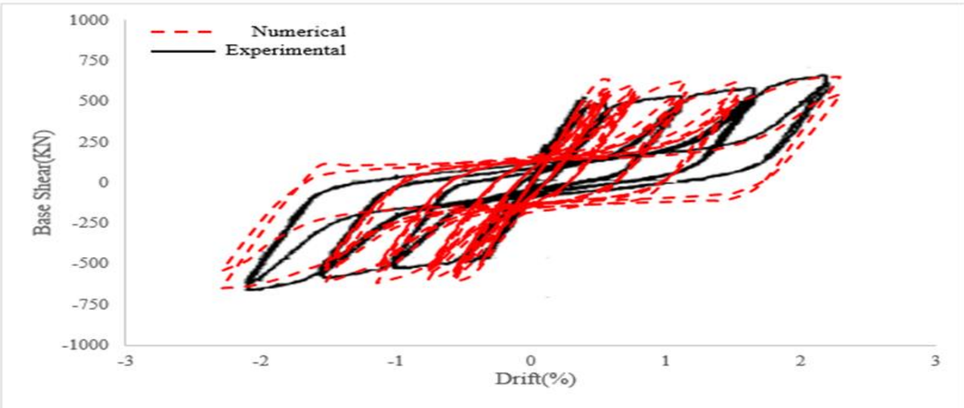

Fig 4 - Comparison between experimental[28] and numerical cyclic curves

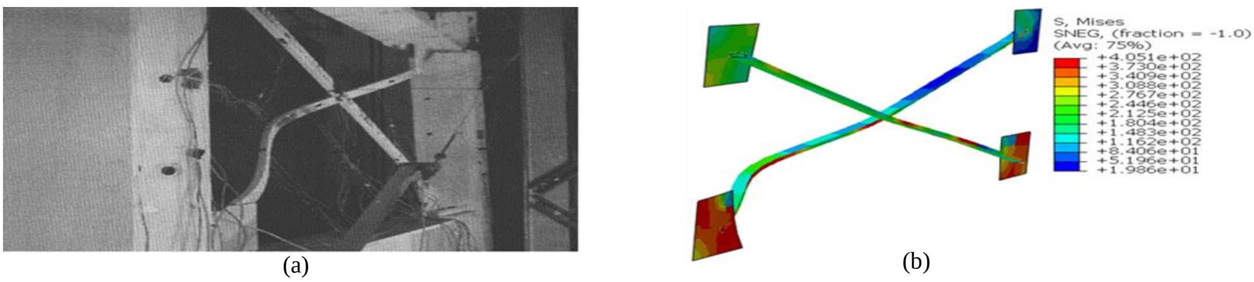

Fig 5 - The results of validation of the experimental sample of the concentrically bracing frame; (a) buckling of the bracing member of the experimental sample[28]; (b) buckling of the bracing member of the numerical sample

2.5.2 Validation of the Link Beam

In order to validate the Vertical Link Beam(VLB) modeling, the results of specimen 9-RLP, one of the link beams tested by Okazaki et al.[29], were used for the modeling in the Abaqus software[23]. The properties of A992 steel were used to define the materials of the link beam. All nodes on the left end of the link beam were closed against rotations in all directions. Moreover, cyclic loading was applied in the vertical direction to the right end of the link beam. According to the results, a constant shear force and equal moments on the two ends were formed during the cyclic loading, and no axial force was created along the link beam. In order for precise simulation of the behavior of the link beam in the software, the loading was applied in accordance with the design principles of AISC[24]. Fig. 6 makes a comparison between the cyclic curves of the experimental specimen and the numerical model. As can be seen, the results are close, and the maximum shear values in the numerical and experimental models are 780.92 and 727.85 kN, respectively, indicating a small difference of 7%. Moreover, Fig. 7 depicts the deformation and yield values in different sections of the link beam, such as the end section of the flange where buckling occurred.

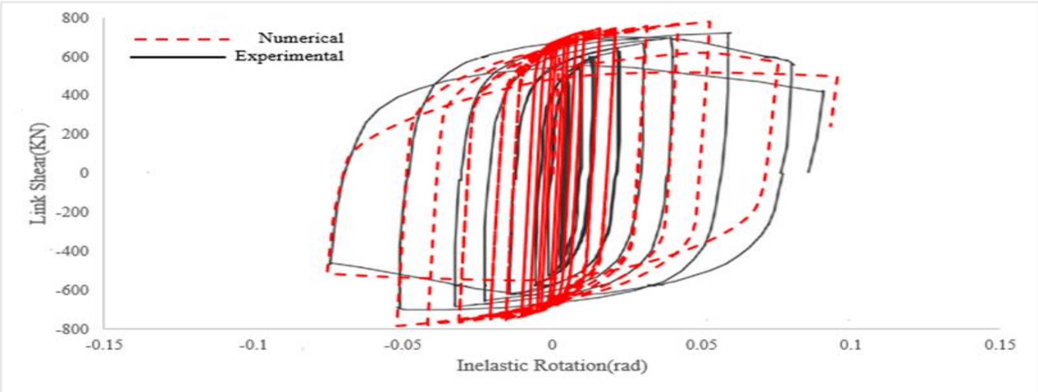

Fig 6 - Comparison between experimental[29] and numerical cyclic curves

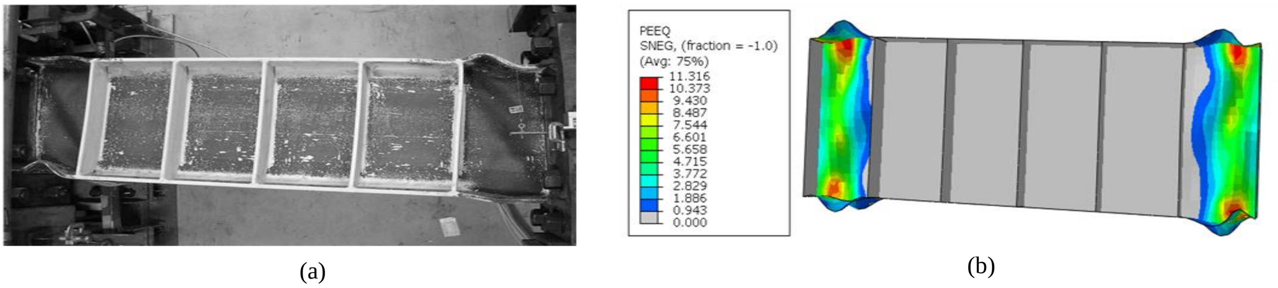

Fig 7 - The results of validation of the experimental sample of the Link Beam; (a) deformed geometry of the experimental sample[29]; (b) deformed geometry of the numerical sample

3. Results

3.1 Monotonic Loading

The pushover analysis of the models under monotonic loading up to the drift of 4% was performed in the Abaqus software[23]. Fig. 8 makes a comparison between the load-displacement curves of model 1 (base model) and models 8 and 9. According to the figure 8, the curve of the model with no VLB has very high stiffness. After a very low displacement, the strength of the model has abruptly declined, which can be due to the formation of plastic hinges and buckling in the bracing members. Such a behavior is not observed in the specimens equipped with VLBs. According to Fig. 8, using VLBs in the X-braced frames (models 8 and 9) has reduced the base shear and elastic stiffness compared to the X-braced frame without any VLB (model 1). This has occurred due to the larger energy dissipation by the Vertical Link Beam.

Furthermore, according to the load-displacement curves shown in Fig. 8, models 8 and 9 have equal elastic stiffness and base shear. Using no stiffeners in model 8 has only resulted in more reduction in the ultimate base shear. Fig. 9 makes a comparison between the nonlinear deformations with the corresponding plastic strain distribution criterion in the main members of the structure in different models. As can be seen in the figure, in the models equipped with VLBs (models 8 and 9), the nonlinear deformation of the main members of the structure, such as bracing members, has declined, and no buckling has occurred in them due to the yielding of the Vertical Link Beam web.

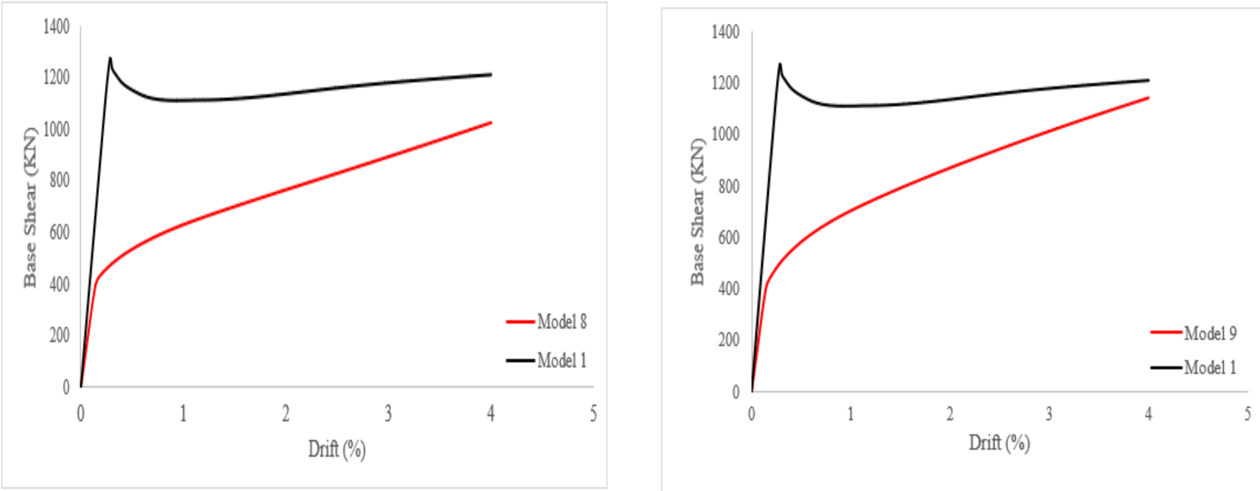

Fig 8 - Comparison of load-displacement curves of pushover analysis

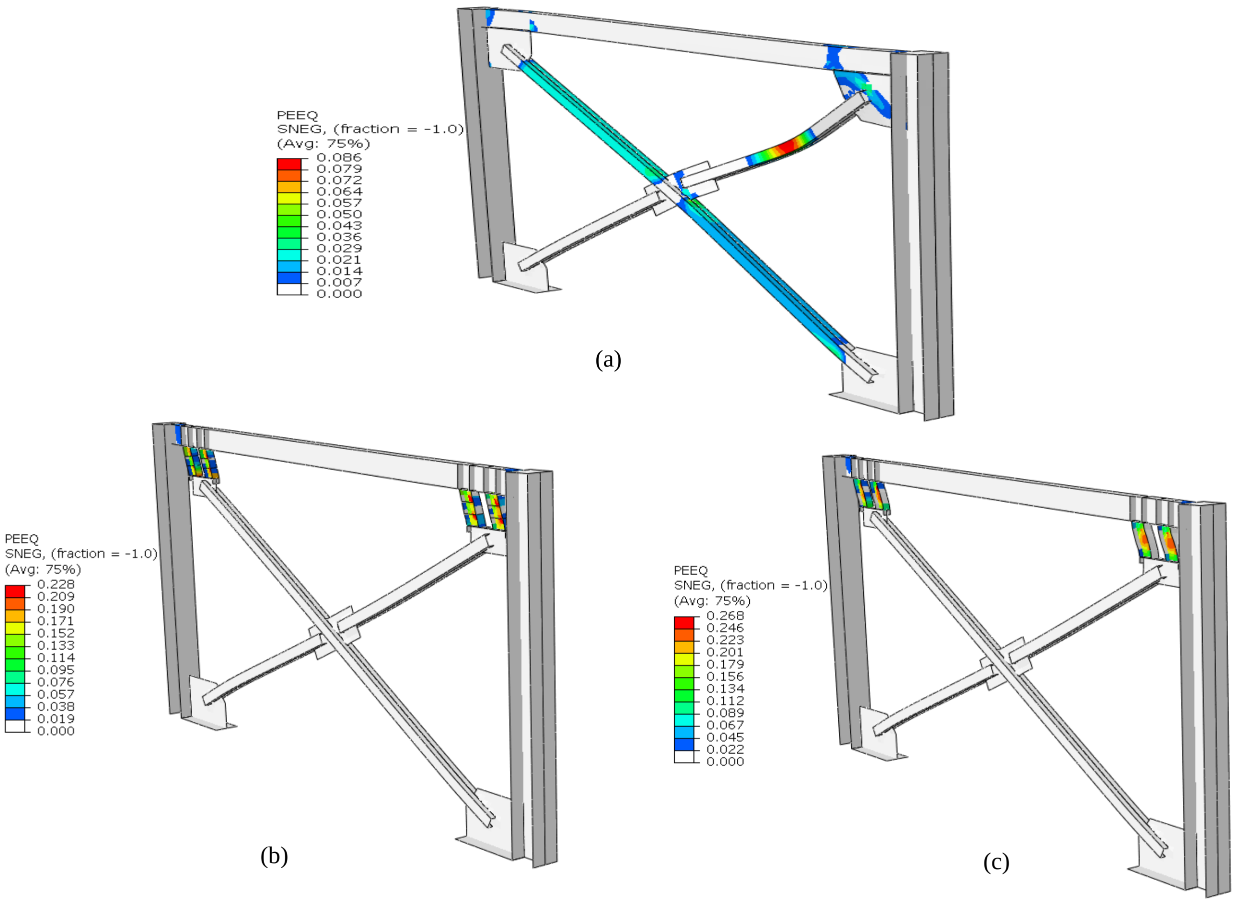

Fig 9 - Comparison of equivalent plastic strain of models; (a) model 1; (b) model 8; (c) model 9

Table 2 summarizes the results obtained from monotonic loading on the models with and without VLBs. The results include yield base shear, ultimate base shear, elastic stiffness, and ductility. According to the table, a remarkable reduction has occurred in the elastic stiffness of the models with VLBs. The reduction is 29-67% compared to the model without any VLB (model 1). A reduction is also shown in the yield and ultimate base shear of the models with VLBs. The largest reduction compared to model 1 belongs to the yield base shear and ultimate base shear, being equal to 82% and 52%. Using VLBs in the X-braced frames has also increased the ductility compared to the model without VLB, since the models equipped with VLBs have not experienced base shear reduction under monotonic loading up to the drift of 4%. According to Table 2, the models with VLBs have resulted in almost the same percentages of reduction in the yield base shear. However, the ultimate base shear has declined more by increasing the VLB length and using no stiffeners. Based on the elastic stiffness values shown in Table 2, this parameter has declined with the reduction in the VLB length, while using stiffeners has had no effect on it. Furthermore, the ductility has experienced a larger rise by reducing the VLB length and using no stiffeners. Based on the results provided in Table 2, with the reduction in the stiffness and strength of the specimens with VLBs and the reduction in the nonlinear deformations shown in Fig. 9, no buckling has occurred in the bracing members, and the VLB has improved the behavior of these members under monotonic loading.

Table 2 - Summary of pushover analysis results

Models	Type of VLB	Specifications of specimens	V_y (KN)	V_y Reduction (%)	V_u (KN)	V_u Reduction (%)	K_e (KN/m)	K_e Reduction (%)	μ
Model 1	-	**XBF**	1187.90	-	1273.74	-	149019.83	-	1.08
Model 2	Single	**XBF-VLB(S)**	213.40	82.04	811.94	36.26	80313.19	46.11	32.73
Model 3		**XBF-VLB(S)**	225.56	81.01	907.50	28.75	75048.74	49.64	28.24
Model 4		**XBF-VLB(S)**	220.55	81.43	604.90	52.51	49800.51	66.58	20.03
Model 5		**XBF-VLB(S)**	227.03	80.89	665.17	47.78	51263.75	65.60	18.26
Model 6	Pair	**XBF-VLB(P)**	426.71	64.08	1263.80	0.78	104590.89	29.81	22.19
Model 7		**XBF-VLB(P)**	428.16	63.96	1300.67	-	105771.14	29.02	20.03
Model 8		**XBF-VLB(P)**	416.62	64.93	1025.75	19.47	83754.03	43.80	19.40
Model 9		**XBF-VLB(P)**	423.98	64.31	1143.67	10.21	85384.81	42.70	17.74
Model 10	Wide	**XBF-VLB(W)**	418.33	64.78	1095.37	14.00	102536.77	31.19	22.59
Model 11		**XBF-VLB(W)**	432.83	63.56	1301.57	-	97736.90	34.41	20.36
Model 12		**XBF-VLB(W)**	412.20	65.30	854.56	32.91	80196.44	46.18	19.11
Model 13		**XBF-VLB(W)**	419.02	64.73	1038.08	18.50	78847.78	47.09	17.74

3.2 Cyclic Loading

The nonlinear static analysis of the base model of the X-braced frame (model 1), along with the models equipped with VLBs, whose properties are presented in Table 1, was performed under the loading protocol of the AISC[24] in the Abaqus software[23]. The cyclic loading results included cyclic curves, damage, von Mises stress, and energy dissipation.

3.2.1 Comparison Between Cyclic Curves

According to Fig. 10, which makes a comparison between the cyclic curves of models 1, 8, and 9, in the model without any VLB (model 1), an abrupt reduction in the stiffness and strength of the X-braced frame is observed due to the buckling of the bracing members under the cyclic loading, like what was observed under monotonic loading. According to Fig. 10, the ultimate base shear in models 1, 8, and 9 equals 1298.77, 653.99, and 775.59 kN, respectively, indicating a 40-50% reduction in models 8 and 9 compared to model 1. The cyclic curves of models with VLBs (models 8 and 9) also reveal higher energy dissipation and ductility compared to the model without any VLB (model 1). Unlike in the base model (model 1), in models 8 and 9, neither buckling in bracing members nor abrupt reduction in stiffness and strength of the X-braced frame is observed. Moreover, the increasing trend of stiffness and strength continues at larger drifts. This indicates that these models can resist more cycles and have a more stable behavior before the buckling of the bracing members and strength and stiffness reduction.

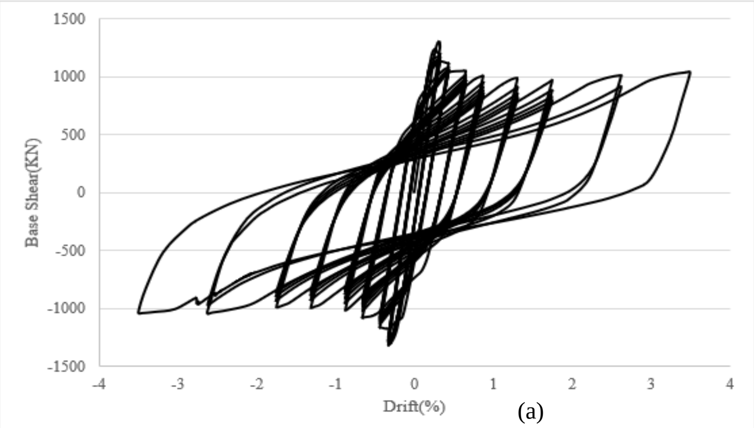

(a)

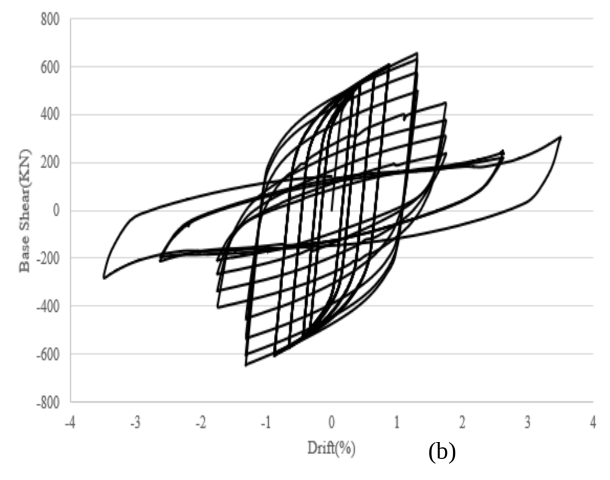

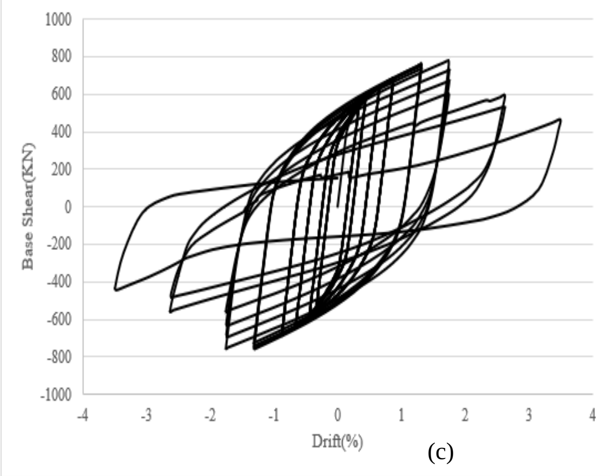

Fig. 10 - Comparison of load-displacement curves of cyclic analysis; (a) model 1; (b) model 8; (c) model 9

According to Table 3, using no stiffeners in the VLB has resulted in a larger reduction in the ultimate base shear of the models with VLBs. However, the change in Vertical Link Beam length has not affected the ultimate base shear. The lowest values of ultimate base shear in the models with single, double, and wide VLBs are 353.54, 653.99, and 489.04 kN, respectively, showing a 50-73% reduction compared to the model without any VLB. According to Table 3, changes in the properties of the VLB, such as stiffeners or length of the link, have not influenced the yield base shear of the models with single, double, and wide VLBs. Furthermore, the lowest values of yield base shear in the models with single, double, and wide VLBs are 220.47, 422.29, and 420.41 kN, respectively, showing a 65-82% reduction compared to the model without any VLB. According to the values of base shear in the moments of the formation of the first and last plastic hinges in the models with VLBs, in the model with a single VLB, the reduction in the base shear has been larger. Furthermore, given the ultimate drifts of the models with VLBs, it can be concluded that the bracing members have experienced nonlinear deformations and damages at larger drifts, and the X-braced frames have been subjected to strength reduction and instability at larger displacements compared to the model without any VLB (model 1). For instance, among the models with double VLBs, the one with stiffeners and a link length of 30 cm has almost 5.5 times larger ultimate drift than the model without any VLB. The reduction in the drifts corresponding with the emergence of the first plastic hinge in the models with VLBs indicates the yield of the VLB at smaller displacements, preventing the yield of the main members of the X-braced frame, such as bracing members. According to the results shown in Table 3, using VLBs has increased the ductility of the X-braced frames. As a result, the high stiffness of the system has declined, and no buckling is observed in the bracing members.

Table 3 - Summary of cyclic analysis results

Models	**Type of VLB**	**Specifications of samples**	**Base Shear (KN)**				**Drift (%)**		**Stiffness (KN/m)**		**Ductility**
			plastic hinges	**Reduction (%)**	**Max**	**Reduction (%)**	**plastic hinges**	**Max**	**K_e**	**Reduction (%)**	**μ**
Model 1	**-**	XBF	1208.36	-	1298.77	-	0.26	0.32	148493.15	-	1.22
Model 2	**Single**	XBF-VLB(S)	226.82	81.23	361.61	72.16	0.11	0.87	65206.27	56.09	7.80
Model 3		XBF-VLB(S)	234.79	80.57	433.41	66.63	0.11	0.87	67323.30	54.66	7.78
Model 4		XBF-VLB(S)	220.47	81.75	353.54	72.78	0.14	1.31	49866.44	66.42	9.19
Model 5		XBF-VLB(S)	229.85	80.98	428.03	67.04	0.15	1.31	49430.97	66.71	8.75
Model 6	**Pair**	XBF-VLB(P)	422.29	65.05	676.96	47.88	0.13	0.87	106546.15	28.25	6.81
Model 7		XBF-VLB(P)	447.25	62.99	773.44	40.45	0.14	0.87	101161.24	31.87	6.14
Model 8		XBF-VLB(P)	426.18	64.73	653.99	49.65	0.17	1.30	78576.79	47.08	7.46
Model 9		XBF-VLB(P)	439.46	63.63	775.59	40.28	0.18	1.74	78704.89	47.00	9.65
Model 10	**Wide**	XBF-VLB(W)	433.14	64.16	566.15	56.41	0.15	0.87	93147.74	37.27	5.83
Model 11		XBF-VLB(W)	438.81	63.69	701.47	45.99	0.15	0.87	94368.39	36.45	5.83
Model 12		XBF-VLB(W)	420.41	65.21	489.04	62.35	0.18	0.87	75293.85	49.29	4.86

Model 13	XBF-VLB(W)	424.57	64.86	697.23	46.32	0.18	1.31	75791.00	48.96	7.23

3.2.2 Damage Parameter and Von Mises Stress

Fig. 11 demonstrates the damage parameter with the ductile damage criterion for models 1, 8, and 9. According to the figure 11, the bracing members in the model without any VLB (model 1) have been damaged, undergone buckling, and failed under cyclic loading. However, in models with VLBs (models 8 and 9), the damage has been much smaller, and most of the nonlinear deformation has occurred in the VLBs' web. The yield of the VLBs has prevented the buckling of the bracing members, which have not failed at drifts larger than those of the base model. Furthermore, according to Fig. 12, in the Vertical Link Beam without stiffeners (model 8), the link's web has mostly experienced nonlinear deformation and damage, while its flange has undergone considerable deformation, which results in instability and lower performance of the system at larger drifts.

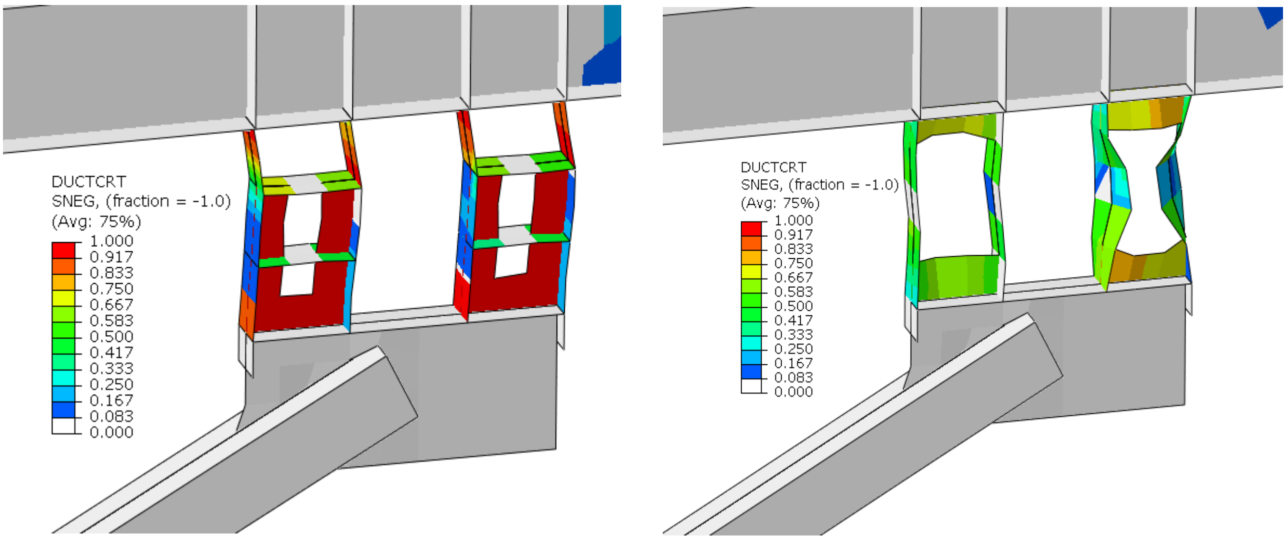

(a) (b)

Fig. 11 - Distribution of damage in VLBs with and without stiffeners; (a) model 8; (b) model 9

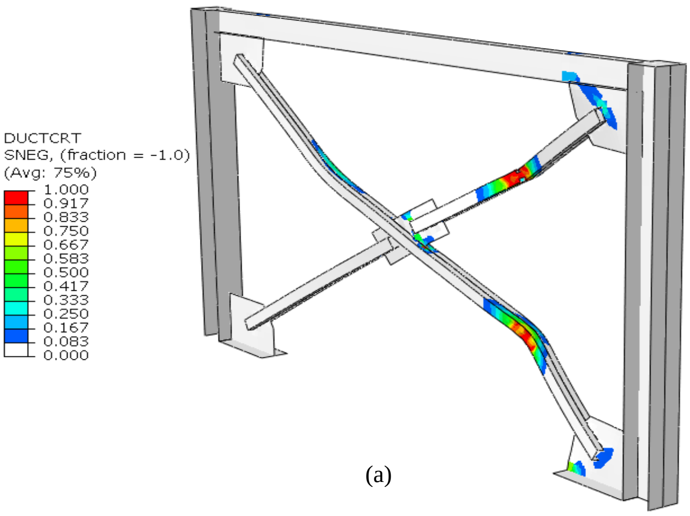

(a)

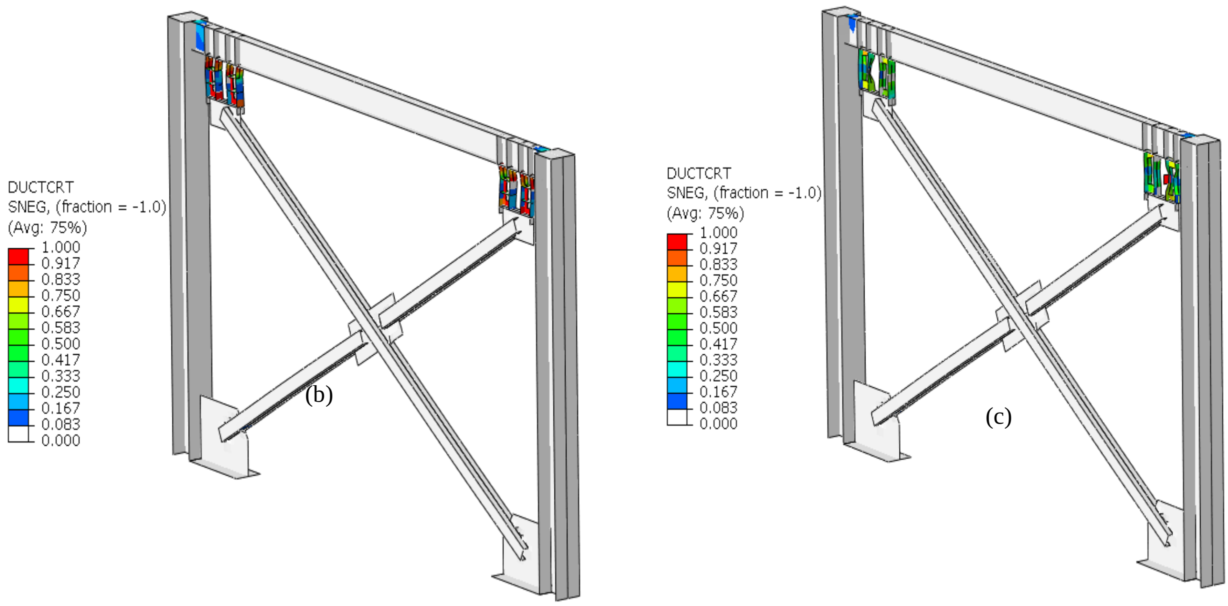

Fig. 12 - Comparison of damage of models; (a) model 1; (b) model 8; (c) model 9

The von Mises stress is a crucial parameter to compare the performance of the models with VLBs with that of model 1 (without any VLB). Table 4 lists the ultimate von Mises stress values of the structure's main members, i.e., beams, columns, and bracing members, in models with and without VLBs. It also provides the ratio of the ultimate von Mises stress to the yield stress of A36 steel (268 MPa) for the main members of the base model and the models with VLBs. The ultimate von Mises stress reduction in the bracing members of the models with VLBs equals 33%, which prevents buckling. Unlike in bracing members, in beams and columns of the models with VLBs, no reduction is observed in the ultimate von Mises stress. Fig. 13 is a diagram for better comparison and evaluation of the reduction in the ratio of the ultimate von Mises stress in bracing members to the yield stress of A36 steel. As can be seen, while using VLBs has reduced the von Mises stress in these members, in none of the models, the bracing members have remained within their elastic zone.

Table 4 - Maximum Von-Mises stress value in structural members

Models	**Type of VLB**	**Specifications of samples**	**Beam**		**Columns**		**Braces**		
			Von-Mises (MPa)	Ratio	Von-Mises (MPa)	Ratio	Von-Mises (MPa)	Ratio	Reduction (%)
Model 1	-	XBF	325.3	1.210	293.4	1.091	487.7	1.814	-
Model 2	Single	XBF-VLB$_{(S)}$	332	1.235	283.6	1.055	333.6	1.241	31.597
Model 3		XBF-VLB$_{(S)}$	328	1.220	283.3	1.054	328	1.220	32.746
Model 4		XBF-VLB$_{(S)}$	317	1.179	285.7	1.062	328.9	1.223	32.561
Model 5		XBF-VLB$_{(S)}$	320	1.190	284.2	1.057	330.4	1.229	32.253
Model 6	Pair	XBF-VLB$_{(P)}$	333.4	1.240	288.2	1.072	338.4	1.258	30.613
Model 7		XBF-VLB$_{(P)}$	331.6	1.233	281.1	1.045	333.7	1.241	31.577
Model 8		XBF-VLB$_{(P)}$	325.9	1.212	283.8	1.055	329.1	1.224	32.520
Model 9		XBF-VLB$_{(P)}$	332.2	1.235	281.2	1.046	335.6	1.248	31.187
Model 10	Wide	XBF-VLB$_{(W)}$	335.2	1.247	280.9	1.045	334.6	1.244	31.392
Model 11		XBF-VLB$_{(W)}$	331	1.231	286.2	1.064	332	1.235	31.925
Model 12		XBF-VLB$_{(W)}$	321.6	1.196	283.8	1.055	333.4	1.240	31.638
Model 13		XBF-VLB$_{(W)}$	334.5	1.244	281.5	1.047	334.4	1.244	31.433

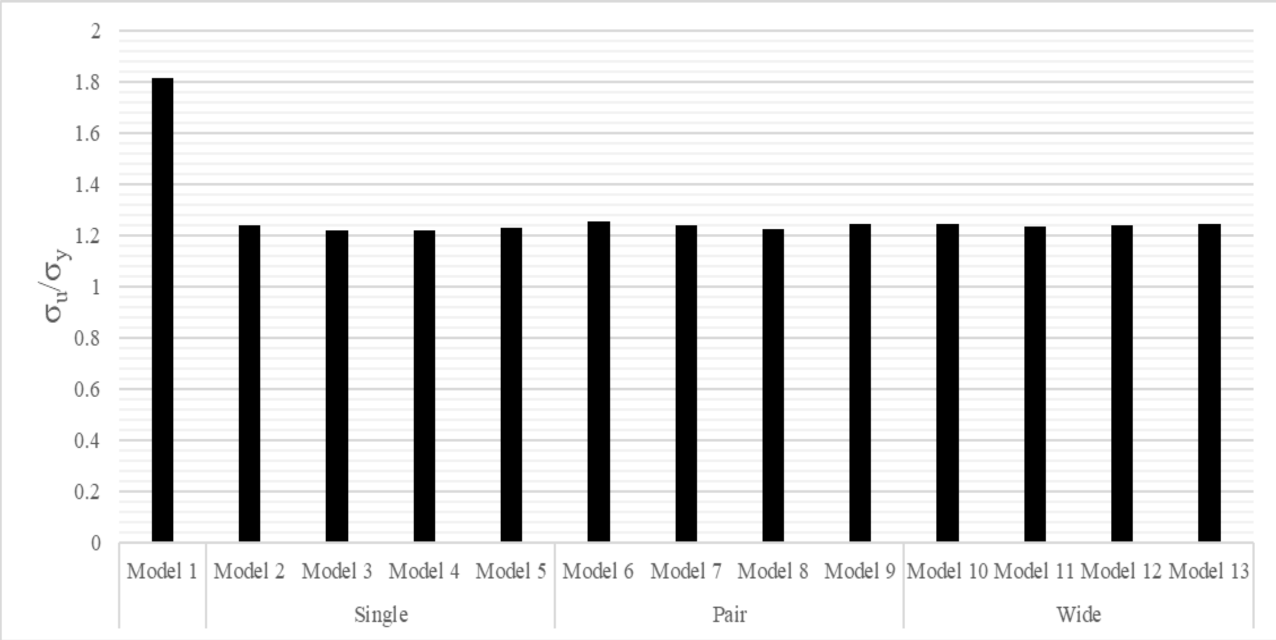

Fig. 13 - The ratio of maximum and yield stress

3.2.3 Dissipated Energy

The value of dissipated energy is another important factor in indicating the performance of earthquake-resistant steel structures. According to the literature, this parameter almost equals the area confined in the cyclic curve of a structural system. Since steel has ductile behavior, and the largest area under the stress-strain curve of steel belongs to the plastic or nonlinear behavior, this area has a larger share of dissipated energy compared to the elastic or linear area in steel structures. The Abaqus software's output of internal dissipated energy, which equals the total energy dissipated, i.e., the dissipated strain and plastic energy, is used to better demonstrate the energy dissipated in the models with VLBs. According to Table 3, in the base model (model 1), the bracing members have buckled at very low drifts, given their remarkable stiffness. As a result, the seismic load-bearing system no longer performs properly and cannot show suitable strength against cyclic loads. However, in the models with VLBs, the proper performance of the system continues at more loading cycles without any buckling or abrupt stiffness reduction in the bracing members. Therefore, for all models, the total dissipated energy is considered the energy dissipated at the drift corresponding with the buckling of the bracing members. Fig. 14 compares the total energy dissipation of the models with and without VLBs.

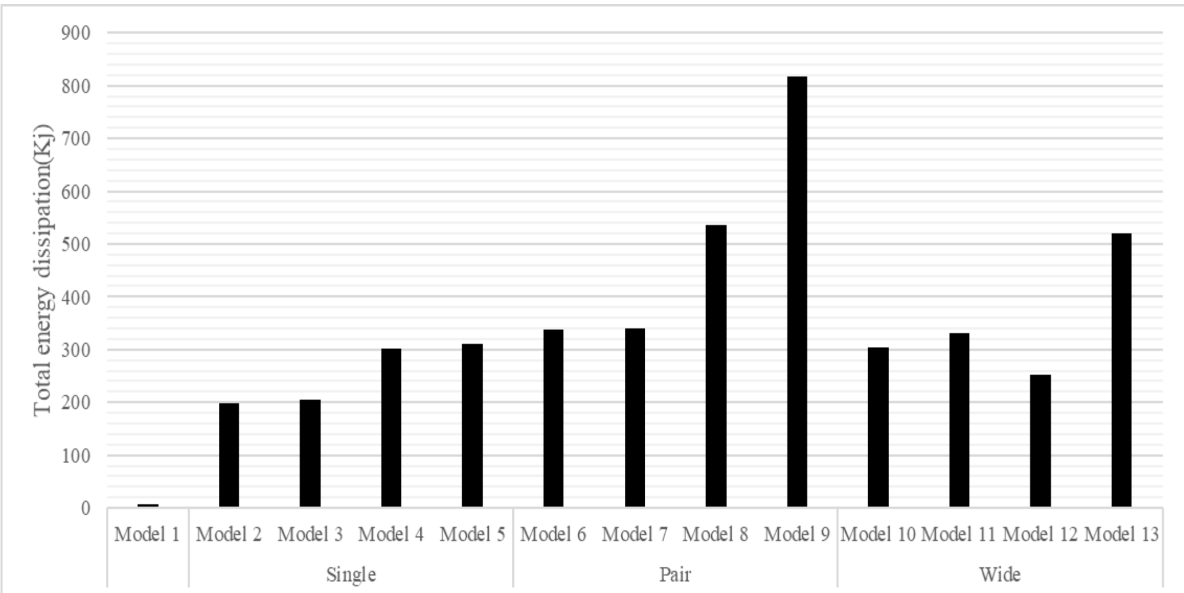

Fig. 14 - Total Dissipated energy for all models

According to the figure 14, the total dissipated energy in the model with no VLBs (model 1) is much lower than in the models with VLBs. The reason is that in the X-braced frames with VLBs, the proper performance of the Vertical link beam in dissipating the energy caused by the cyclic loading has prevented stiffness reduction or buckling in the bracing members, and the system has been able to resist larger drifts compared to the base model. The highest total energy dissipated in the models with single, double, and wide VLBs equals 310.24, 816.923, and 520.797 kJ, respectively. Moreover, according to Fig. 15, which depicts the energy dissipated by the VLBs in the models, more than 90% of the energy produced from cyclic loading has been dissipated by the VLBs, preventing buckling or nonlinear deformations in the bracing members, indicating the stable performance of the models compared to the base model.

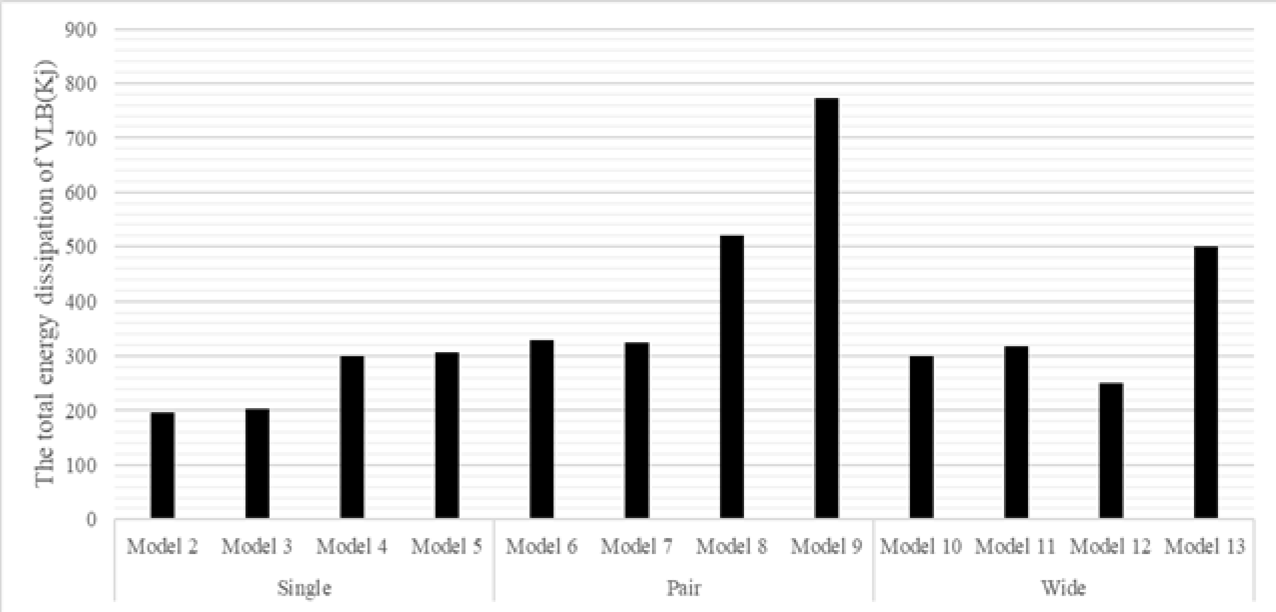

Fig. 15 - Total Dissipated energy of VLBs

4. Conclusions

The present study investigated the behavior of X-braced frames with Vertical link beam (XBF-VLB) under monotonic and cyclic loading using numerical methods in the Abaqus finite element software. The studied models included a X-braced frame without any VLB (the base model), along with models with single, double, and wide VLBs. Different properties of VLBs, such as stiffeners and length of links, were examined. Various parameters, including elastic stiffness, yield base shear, ductility, ultimate base shear, equivalent plastic strain distribution, cyclic curves, von Mises stress, and damage, were also evaluated to study the performance of X-braced frames under monotonic and cyclic loading. The following summarizes the obtained results.

1) The VLB's performance in the X-braced frame under monotonic and cyclic loading reduced the stiffness and strength of the models by 29-69% compared to the base model. This reduction prevented the abrupt buckling of the bracing members in the models with VLBs. The monotonic and cyclic curves of these models had an increasing trend in strength and stiffness, and no abrupt reduction caused by the buckling of the main members was observed. Furthermore, compared to the base model, the ones with VLBs resisted strength reduction at larger drifts, indicating their stable performance. The strength and stiffness reduction were larger in the models with single VLBs compared to the other models with VLBs.

2) The pushover analysis revealed a reduction in the yield and ultimate base shear in the models with VLBs under monotonic loading. The largest reduction in the yield and ultimate base shear compared to the base model equaled 82% and 52%, respectively. The corresponding values were 82% and 73%, respectively, under cyclic loading.

3) The evaluation of the equivalent plastic strain distribution in the analysis of the monotonic loading, which indicated the nonlinear deformation of the members in the X-braced frame, showed that the distribution was very low in the bracing members of the models with VLBs and did not lead to the buckling of these members.

4) The pushover and cyclic analysis results of the models with VLBs indicated increased ductility caused by energy dissipation and proper performance of the VLBs compared to the base model. Under monotonic loading, the models with single VLBs and no stiffeners showed several times larger ductility than the base model.

5) Evaluating the ultimate stress and its ratio to the yield stress of the A36 steel in the main members of the models with VLBs showed that using VLBs resulted in 33% lower ultimate stress in the bracing members, preventing buckling. Assessment of the ductile damage parameter also revealed that the bracing members entered the damage zone and failed in the base model.

6) By evaluating the total energy dissipated in the models, it was found that using VLBs enhanced the system's performance and increased the energy dissipation compared to the base model.

According to the results mentioned, using VLBs improved the performance of the X-braced frames under monotonic and cyclic loading, preventing the buckling of the bracing members at small displacements due to the notable stiffness of this system.

Acknowledgement

The authors would like to thank Department of Civil Engineering, Qazvin Branch, Islamic Azad University, Qazvin, Iran for allowing to conduct this research.

Reference

A. AISC, "Seismic provisions for structural steel buildings," ed: Chicago, 2010.

A. Daneshmand and B. H. Hashemi, "Performance of intermediate and long links in eccentrically braced frames," *Journal of Constructional Steel Research,* vol. 70, pp. 167-176, 2012.

C. W. Roeder and E. P. Popov, "Eccentrically braced steel frames for earthquakes," *Journal of the Structural Division,* vol. 104, no. 3, pp. 391-412, 1978.

D. Dubina, A. Stratan, and F. Dinu, "Dual high ‐ strength steel eccentrically braced frames with removable links," *Earthquake Engineering & Structural Dynamics,* vol. 37, no. 15, pp. 1703-1720, 2008.

D. Özhendekci and N. Özhendekci, "Effects of the frame geometry on the weight and inelastic behaviour of eccentrically braced chevron steel frames," *Journal of Constructional Steel Research,* vol. 64, no. 3, pp. 326-343, 2008.

E. Miranda and V. V. Bertero, "Evaluation of strength reduction factors for earthquake-resistant design," *Earthquake spectra,* vol. 10, no. 2, pp. 357-379, 1994.

E. Nastri, R. Montuori, and V. Piluso, "Seismic design of MRF-EBF dual systems with vertical links: EC8 vs plastic design," *Journal of Earthquake Engineering,* vol. 19, no. 3, pp. 480-504, 2015.

J. D. Aristizabal-Ochoa, "Disposable knee bracing: improvement in seismic design of steel frames," *Journal of Structural engineering,* vol. 112, no. 7, pp. 1544-1552, 1986.

K.-C. Lin, C.-C. J. Lin, J.-Y. Chen, and H.-Y. Chang, "Seismic reliability of steel framed buildings," *Structural safety,* vol. 32, no. 3, pp. 174-182, 2010.

L. Mastrandrea and V. Piluso, "Plastic design of eccentrically braced frames, I: Moment–shear interaction," *Journal of Constructional Steel Research,* vol. 65, no. 5, pp. 1007-1014, 2009.

M. Bosco and P. Rossi, "Seismic behaviour of eccentrically braced frames," *Engineering Structures,* vol. 31, no. 3, pp. 664-674, 2009.

M. Naghipour, N. Javadi, and A. Naghipour, "Investigation of RBS connection ductility in eccentrically braced frame," *Procedia engineering,* vol. 14, pp. 743-752, 2011.

M.-T. Sam, T. Balendra, and C.-Y. Liaw, "Earthquake-resistant steel frames with energy dissipating knee elements," *Engineering Structures,* vol. 17, no. 5, pp. 334-343, 1995.

O. C. Celik, J. W. Berman, and M. Bruneau, "Cyclic testing of braces laterally restrained by steel studs," *Journal of Structural Engineering,* vol. 131, no. 7, pp. 1114-1124, 2005.

P. Rossi and A. Lombardo, "Influence of the link overstrength factor on the seismic behaviour of eccentrically braced frames," *Journal of Constructional Steel Research,* vol. 63, no. 11, pp. 1529-1545, 2007.

P. W. Richards and C.-M. Uang, "Effect of flange width-thickness ratio on eccentrically braced frames link cyclic rotation capacity," *Journal of structural engineering,* vol. 131, no. 10, pp. 1546-1552, 2005.

R. Aghlara and M. M. Tahir, "A passive metallic damper with replaceable steel bar components for earthquake protection of structures," *Engineering structures,* vol. 159, pp. 185-197, 2018.

R. Aghlara, M. M. Tahir, and A. B. Adnan, "Experimental study of Pipe-Fuse Damper for passive energy dissipation in structures," *Journal of Constructional Steel Research,* vol. 148, pp. 351-360, 2018.

R. Montuori, E. Nastri, and V. Piluso, "Theory of plastic mechanism control for eccentrically braced frames with inverted Y-scheme," *Journal of Constructional Steel Research,* vol. 92, pp. 122-135, 2014.

R. Montuori, E. Nastri, and V. Piluso, "Rigid-plastic analysis and moment–shear interaction for hierarchy criteria of inverted Y EB-Frames," *Journal of Constructional Steel Research,* vol. 95, pp. 71-80, 2014.

R. Montuori, E. Nastri, and V. Piluso, "Theory of Plastic Mechanism Control for MRF–EBF dual systems: Closed form solution," *Engineering Structures,* vol. 118, pp. 287-306, 2016.

S. M. ZAHRAEI and A. Moslehitabar, "Cyclic behaviour of steel braced frames having shear panel system," 2006.

S. M. Zahrai, M. Pirdavari, and H. M. Farahani, "Evaluation of hysteretic behavior of eccentrically braced frames with zipper-strut upgrade," *Journal of Constructional Steel Research,* vol. 83, pp. 10-20, 2013.

S. S. Askariani, S. Garivani, and A. A. Aghakouchak, "Application of slit link beam in eccentrically braced frames," *Journal of Constructional Steel Research,* vol. 170, p. 106094, 2020.

T. Balendra, E.-L. Lim, and S.-L. Lee, "Ductile knee braced frames with shear yielding knee for seismic resistant structures," *Engineering Structures,* vol. 16, no. 4, pp. 263-269, 1994.

T. Okazaki and M. D. Engelhardt, "Cyclic loading behavior of EBF links constructed of ASTM A992 steel," *Journal of constructional steel Research,* vol. 63, no. 6, pp. 751-765, 2007.

U. s. G. ABAQUS and T. Manual, "Ver. 6.8, ABAQUS," *Inc., Providence, RI*, 2008.

W. Thornton, "On the analysis and design of bracing connections," in *Proceedings AISC National Steel Construction Conference*, 1991, pp. 26-1.

X. Ma, E. Borchers, A. Pena, H. Krawinkler, S. Billington, and G. Deierlein, "Design and behavior of steel shear plates with openings as energy-dissipating fuses," *John A. Blume Earthquake Engineering Center Technical Report,(173)*, 2010.